



Oxidation of low-molecular weight organic compounds in cloud droplets: development of the JAMOC chemical mechanism in CAABA/MECCA (version 4.5.0gmdd)

Simon Rosanka¹, Rolf Sander², Andreas Wahner¹, and Domenico Taraborrelli¹

¹Forschungszentrum Jülich GmbH, Institute of Energy and Climate Research, IEK-8: Troposphere, Jülich, Germany

²Atmospheric Chemistry Department, Max-Planck Institute of Chemistry, Mainz, Germany

Correspondence: Simon Rosanka (s.rosanka@fz-juelich.de)

Abstract. The Jülich Aqueous-phase Mechanism of Organic Chemistry (JAMOC) is developed and implemented in the Module Efficiently Calculating the Chemistry of the Atmosphere (MECCA, version 4.5.0gmdd¹). JAMOC is an explicit in-cloud oxidation scheme for oxygenated volatile organic compounds (OVOCs), suitable for global model applications. It is based on a subset of the comprehensive CLoud Explicit Physico-chemical Scheme (CLEPS, version 1.0). The phase transfer of species containing up to ten carbon atoms is included, and a selection of species containing up to four carbon atoms reacts in the aqueous-phase. In addition, the following main advances are implemented: (1) simulating hydration and dehydration explicitly, (2) taking oligomerisation of formaldehyde, glyoxal and methylglyoxal into account, (3) adding further photolysis reactions, and (4) considering gas-phase oxidation of new outgassed species. The implementation of JAMOC in MECCA makes a detailed in-cloud OVOC oxidation model readily available for box as well as for regional and global simulations that are affordable with modern supercomputing facilities. The new mechanism is tested inside the box-model Chemistry As A Boxmodel Application (CAABA), yielding reduced gas-phase concentrations of most oxidants and OVOCs except for the nitrogen oxides.

1 Introduction

Aqueous-phase chemistry in cloud droplets differs significantly from gas-phase chemistry, mainly due to enhanced photolysis based on scattering effects within cloud droplets (Bott and Zdunkowski, 1987; Mayer and Madronich, 2004), faster reaction rates, and ion reactions that do not occur in the gas-phase (Herrmann, 2003; Epstein and Nizkorodov, 2012). Moreover, nitrogen monoxide (NO) to nitrogen dioxide (NO₂) conversion by peroxy radicals (RO₂) essentially does not take place in liquid droplets because NO is insoluble. Compared to gas-phase chemistry, knowledge of aqueous-phase chemistry still suffers from large uncertainties and most global models only include very limited representations (Ervens, 2015). In the gas-phase, oxygenated volatile organic compounds (OVOCs) are mainly oxidised during daytime by hydroxyl radical (OH). Herrmann et al. (2015) showed that the partitioning and oxidation of OVOCs in cloud droplets significantly influence the OH budget. When

¹ The name of this version indicates that it is used for the interactive discussion in GMDD. If necessary, bug fixes can still be made. We plan to release the final version CAABA/MECCA-4.5.0 together with the final paper in GMD.



performing global studies, it is thus desirable to include their in-cloud oxidation. However, most global models include only the uptake of a few soluble compounds, their acid-base equilibria, and the oxidation of sulfur dioxide (SO_2) via ozone (O_3) and hydrogen peroxide (H_2O_2) (Ervens, 2015, Table 1). The explicit oxidation of OVOCs is currently not considered in any
25 global model with one exception though limited to species containing one carbon atom (Tost et al., 2006). Mouchel-Vallon et al. (2017) recently presented the Cloud Explicit Physico-chemical Scheme (CLEPS, version 1.0), a new complex oxidation scheme coupled to the gas-phase Master Chemical Mechanism (MCM, version 3.3.1, Jenkin et al., 2015). However, their comprehensive mechanism is targeted for box-model applications and is not suitable for global model applications, due to its complexity.

30 In this study, the in-cloud OVOC oxidation scheme Jülich Aqueous-phase Mechanism of Organic Chemistry (JAMOC) is presented. It is based on CLEPS and implemented into the chemistry mechanism Module Efficiently Calculating the Chemistry of the Atmosphere (MECCA). The modular structure of MECCA allows it to be connected to different base models, e.g., to the Chemistry As A Boxmodel Application (CAABA) by Sander et al. (2019), or to the global ECHAM/MESSy Atmospheric Chemistry Model (EMAC) by Jöckel et al. (2010). In this combination, the proposed mechanism closes the gap between
35 box-models and global model applications.

In addition to the new OVOC chemistry, MECCA also contains the gas-phase Mainz Organic Mechanism (MOM, Sander et al., 2019) with an extensive oxidation scheme for isoprene (Taraborrelli et al., 2009, 2012; Nölscher et al., 2014), monoterpene (Hens et al., 2014), and aromatics (Cabrera-Perez et al., 2016). VOCs are oxidised by OH , O_3 and nitrogen trioxide (NO_3), whereas RO_2 react with HO_2 , NO_x , and NO_3 and undergo self- and cross-reactions (Sander et al., 2019).

40 The mechanism of JAMOC is described in Sect. 2, followed by a short description of its implications in the box-model CAABA (Sect. 3). Global implications are analysed in our companion paper (Rosanka et al., 2020). Modelling uncertainties are discussed in Sect. 4 before drawing final conclusions in Sect. 5.

2 The Jülich Aqueous-phase Mechanism of Organic Chemistry (JAMOC)

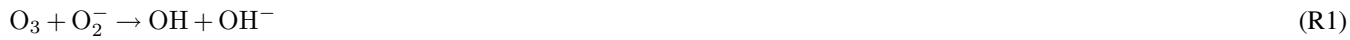
This section provides a general overview of the developed mechanism. For completeness, short summaries of CLEPS are
45 provided, if no significant difference exists between both mechanisms. Figures 1 and 2 give a graphical representation of all parts of the developed mechanism, using glyoxal and oxalic acid as examples. In order to make the mechanism suitable for global models, the number of reactions was reduced in comparison to CLEPS. This was achieved by reducing the number of treated species, i.e. only a selection of species containing up to four carbon atoms react within the aqueous-phase. The phase transfer of species containing up to ten carbon atoms is still represented. In comparison to CLEPS, the mechanism was extended
50 to: (1) simulating hydration and dehydration explicitly, (2) taking oligomerisation for formaldehyde, glyoxal and methylglyoxal into account, (2) adding further aqueous-phase photolysis reactions, and (4) considering the gas-phase photo-oxidation of new outgassed species. The complete aqueous-phase mechanism represents the phase transfer of 368 species, 68 equilibria (acid base and hydration), 402 reactions, and 27 aqueous-phase photolysis reactions. In the gas-phase, 1 photolysis and 18 OH



oxidation reactions are added to MOM. A list of the complete mechanism is available in the supplement (caaba_4.5.0gmdd/
55 manual/meccanism.pdf).

2.1 Inorganic chemistry

The inorganic chemistry for the proposed mechanism is very similar to the inorganic chemistry of the standard aqueous-phase mechanism used in EMAC (Tost et al., 2007; Jöckel et al., 2016) and reactions included in MECCA (e.g. Fenton chemistry), which are not yet implemented in EMAC. In this standard mechanism, the major O_3 sink, the reaction with superoxide anions
60 (O_2^-), is represented as:



In JAMOC, this reaction is updated to the mechanism proposed by Staehelin et al. (1984) with corrections from Staehelin and Hoigné (1985):



65 which includes the implementation of the chemistry of ozonide (O_3^-) and the reaction of O_3 with hydroxide (OH^-).

2.2 Uptake of gaseous species into cloud droplets

The mass transfer of species between the gas- and the aqueous-phase is described following Schwartz (1986) (see Sander, 1999; Tost et al., 2006). The explicit bidirectional phase transfer of 45 carbon-containing species, which explicitly react in the aqueous-phase, is considered (indicated in pink in Fig. 1 and 2). In this model framework, only outgassing depends on Henry's
70 law constants, which are mainly taken from Sander (2015), Burkholder et al. (2015), and sources therein. In order to account for the hydration of aldehydes (for more details see Sect. 2.3), a distinction is made between the apparent Henry's law constant (H^*) and the intrinsic Henry's law constant (H). The latter is calculated by:

$$H = H^* / (1 + K_{hyd}) \quad (1)$$

where K_{hyd} is the ratio between the forward and reverse kinetic rate constant of the hydration equilibrium (see Reaction R3).
75 Table 1 gives an overview of the hydration constants and the apparent Henry's law constants, including the resulting intrinsic Henry's law constants, for all aldehydes. The temperature dependencies of the intrinsic Henry's law constants are assumed to be the same as for the apparent constants. The accommodation constant (α) is known for a few species, if unknown the standard EMAC estimate of 0.1 is used. In addition to the phase transfer of all species that explicitly react in the aqueous-phase, the phase transfer of all soluble MOM species containing up to ten carbon atoms is represented. A list summarising all Henry's
80 law and accommodation constants is available in the supplement (caaba_4.5.0gmdd/tools/chemprop/chemprop.pdf).



2.3 Hydration of carbonyls

Gem-diols are formed when aldehydes (carbonyl compounds) hydrate:



In the new mechanism, 12 carbonyl species undergo hydration (indicated with blue arrows in Fig. 1). The monohydrate of glyoxal undergoes an additional hydration to form its dihydrate. Pseudo-first order rate constants for the hydration and dehydration are mainly obtained from the literature (e.g. Doussin and Monod, 2013). The Henry's law constants for the gem-diols are unknown. Estimates are obtained at 25 °C using the bond method from the United States Environmental Protection Agency Estimation Programs Interface (EPI) Suite (US EPA, 2012).

In CLEPS, acyl peroxy radicals ($\text{RC}(\text{O})(\text{OO})$) are assumed to be in a hydration/dehydration equilibrium similar to their parent aldehydes (Mouchel-Vallon et al., 2017). However, experimental results by Villalta et al. (1996) show that in the case of peroxyacetyl radicals ($\text{CH}_3\text{C}(\text{O})(\text{OO})$) no equilibrium exists. Instead, hydrolysis takes place likely yielding acetic acid ($\text{CH}_3\text{CO}_2\text{H}$) and HO_2 . It is thus assumed that all acyl peroxy radicals undergo hydrolysis following:



with a reaction rate constant of $7.0 \times 10^5 \text{ M}^{-1}\text{s}^{-1}$, as proposed by Villalta et al. (1996).

2.4 Acid dissociation

The dissociation of acids is taken into account following:



which is indicated in green in Fig. 2. The acidity constants (K_a) for most one, two, and three carbon containing acids taken into account in JAMOC, are known from the literature (Rumble, 2020). If unknown, the acidity constants are used as proposed by Mouchel-Vallon et al. (2017). The dissociation and association rate constants are selected such that the equilibrium between dissociation and association is reached quickly, while still avoiding numerical stiffness problems in the numerical integrator.

2.5 Oxidation by OH, NO_3 and other oxidants

In JAMOC, OH and NO_3 are the main oxidants taken into account. Reactions of OVOCs with oxidants are treated as proposed by Mouchel-Vallon et al. (2017). Organic compounds may react in three different ways with OH radicals (Herrmann et al., 2015) each indicated in orange in Fig. 1 and 2. They form an alkyl radical following H-abstraction:





If the organic compound contains a double bond OH-addition is favoured:



With anions like carboxylates electron transfer takes place:



During nighttime, OH radical concentrations are low. The reaction with NO_3 radicals is thus considered to be the main nighttime oxidation pathway. Even though little is known from the literature, this process is still included, since this mechanism is targeted for global model applications. However, as proposed by Mouchel-Vallon et al. (2017), only the H-abstraction leading to alkyl radicals is taken into account for NO_3 reactions (Herrmann et al., 2015):



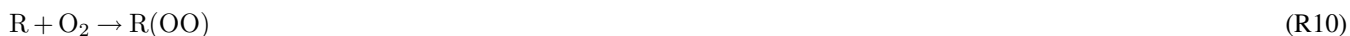
In addition to reactions of organic compounds with OH and NO_3 , reactions with other oxidants are implemented when available from the literature. The oxidants considered here are O_2^- , O_3 , H_2O_2 , CO_3^- , and sulfur containing oxidants (SO_4^- and SO_5^-). For all oxidation reactions, reaction rates and branching ratios are either taken from literature or as proposed by Mouchel-Vallon et al. (2017).

120 2.6 Oligomerization

Self- and cross-reactions leading to oligomers are implemented for formaldehyde, glyoxal, and methylglyoxal. The oligomerization of formaldehyde is implemented following Hahnenstein et al. (1995), in which the methanediol formed from hydrolysis (see Sect. 2.3) reacts with itself and the dimer formed from this self-reaction. Ervens and Volkamer (2010) studied the oligomerization of glyoxal. Here, glyoxal and its hydrates react with the monohydrate to form three oligomers (indicated in green in Fig. 1). The oligomerization of methylglyoxal is assumed to follow the same mechanisms as for glyoxal. However, only the monohydrate of methylglyoxal is taken into account in this mechanism, leading to only two oligomers. Each oligomer is assumed to react with OH, leading to HO_2 , with reaction rate constants that are double for the corresponding (hydrated) monomer.

2.7 Organic radicals

130 Organic radicals are generally treated following Mouchel-Vallon et al. (2017). Alkyl radicals can either form oligomers via self- and cross-reactions (e.g. Lim et al., 2013; Ervens et al., 2015) or undergo O_2 addition:



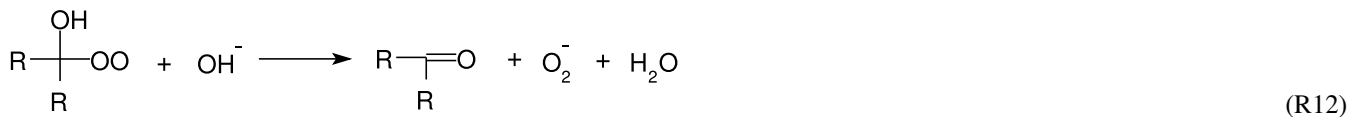


As proposed by Mouchel-Vallon et al. (2017), it is assumed that O_2 addition is the fastest pathway, due to high O_2 concentrations following a fast O_2 saturation in cloud droplets (Ervens, 2015). Thus, oligomerisation of alkyl radicals is not considered
 135 in this mechanism.

Peroxy radicals generally undergo self- or cross-reactions forming short-lived tetroxides that quickly decompose (von Sonntag and Schuchmann, 1997). Due to limited computation resources, only self-reactions are taken into account. Mouchel-Vallon et al. (2017) propose three similarity criteria for the decomposition of tetroxides depending on the peroxy radical: (1) for β -peroxycarboxylic acids ($RC(OO)C(=O)(OH)$) experimental results from Schuchmann et al. (1985) are generalised,
 140 (2) β -hydroperoxyperoxy radicals ($>C(OH)C(OO)<$) are represented according to Piesiak et al. (1984), and (3) β -oxoperoxy radicals ($-COC(OO)<$) are treated based on Zegota et al. (1986) and Poulain et al. (2010). In all cases, branching ratios are rescaled to 100 %. The peroxy radicals undergo HO_2 elimination (von Sonntag, 1987), if the hydroxyl moiety is in the alpha position (α -hydroperoxyperoxy):



145 The generalised corresponding rate constants are used as proposed by Mouchel-Vallon et al. (2017, Table 3), which are based on the work of von Sonntag (1987). In CLEPS, peroxy radicals additionally undergo O_2^- elimination when reacting with OH^- (Zegota et al., 1986; Mouchel-Vallon et al., 2017):



In order to decrease the number of reactions and due to the fast HO_2 elimination, this O_2^- elimination is not considered
 150 explicitly in JAMOC.

Acyl peroxy radicals ($RC(O)(OO)$) are treated like peroxy radicals, as described in Monod et al. (2007), but only form alkoxy radicals. Peroxy radicals that have not explicitly discussed so far are treated following Monod et al. (2007) (Mouchel-Vallon et al., 2017).

155 Mouchel-Vallon et al. (2017) suggest that alkoxy radicals (RO) either undergo a carbon bond scission (Hilborn and Pincock, 1991), if the neighbouring carbon atom is oxygenated:



or an 1-2 hydrogen shift (DeCosta and Pincock, 1989), if the neighbouring carbon atom is not oxygenated:





160 In order to reduce the stiffness of the ODE system and the required computational demand, it is assumed that the following reactions occur instantly and are not explicitly represented in ODE system, if it is the only fate of the respective radical: (1) the O₂ addition to alkyl radicals, (2) the HO₂ elimination of α -hydroxyperoxyxl and (3) the carbon bond scission or 1-2 hydrogen shift of alkoxy radicals.

2.8 Photolysis

165 In general, the photolysis of organic compounds competes with the other oxidation pathways (see Sect. 2.5) and is a major source of OH (indicated in orange in Fig. 1 and 2). The number of photolytic reactions known from literature, of which some are implemented in CLEPS (Mouchel-Vallon et al., 2017), is limited. In JAMOC, the photolysis of additional compounds is taken into account. This includes the photolysis of oxalic acid (HOOCCOOH), which is implemented following Yamamoto and Back (1985) using the ultraviolet absorption spectrum presented in Back (1984). If available, additional photolysis reactions are implemented following Sander et al. (2014). In order to account for scattering effects within cloud droplets (Ruggaber et al., 170 1997), an enhancement factor of 2.33, the same as used in EMACs standard aqueous-phase mechanism for the photolysis of H₂O₂ (Tost et al., 2007; Jöckel et al., 2016), is applied to each photolysis rate.

2.9 Gas-phase oxidation of new species

175 Oxalic acid was not represented in the gas-phase mechanism (i.e. in MOM). The gas-phase oxidation of oxalic acid via OH and its photolysis are implemented, in order to realistically represent oxalic acid in the gas-phase. Similar to the implementation in the aqueous-phase, the photolysis of oxalic acid is implemented following Yamamoto and Back (1985) and Back (1984). In addition, gem-diols (see Sect. 2.3) formed from hydration are transferred to the gas-phase and oxidised via OH (indicated in orange in Fig. 1 and 2). All OH oxidation reaction rates are estimated following the description of Sander et al. (2019).

3 Influence of JAMOC on a single air parcel

180 The implications of the developed mechanism are tested by comparing it to the minimum in-cloud oxidation scheme available in CAABA/MECCA and EMAC. The minimum mechanism only includes the uptake of a few soluble compounds, their acid-base equilibria, and the oxidation of SO₂ via O₃ and H₂O₂ (Jöckel et al., 2006). This minimal mechanism is thus representable for most global models (Ervens, 2015). For both mechanisms, an air parcel is simulated in CAABA taking the same conditions into account: the air parcel is simulated during summer at mid-latitude with a constant temperature of 278 K and relative humidity of 70 %. Table 2 provides a selection of initial mixing ratios and emission fluxes of gas-phase species treated in 185 MOM. The initial conditions are a modified version of the scenario used by Taraborrelli et al. (2009). Within the air parcel, a stable cloud droplet is simulated with a radius of 20 μm and a liquid water content of $3.0 \times 10^{-1} \text{ g L}^{-1}$. CAABA is initialised at 0 UTC and simulates the air parcel for five days in total.

Figure 3 gives an overview of the temporal development of gas-phase concentrations for a selection of species during the simulated daily cycles of 5 days. Comparing the new and the minimum mechanisms, it becomes clear that the new developed



190 mechanism has a significant impact on most trace gases. With the explicit oxidation of many OVOCs, the overall gas-phase
OVOC concentrations are significantly reduced. This reduction is a combined effect from: (1) the in-cloud oxidation of these
OVOCs, and (2) their damped gas-phase production. In the gas-phase, most OVOCs are formed by secondary production
(e.g. oxidation of primarily emitted VOCs). The decrease of the main VOC oxidant (i.e. OH) leads to a reduced oxidation of
primarily emitted VOCs resulting in a reduced gas-phase OVOC formation. The calculated diurnal cycles of OH, HO₂, NO_x,
195 and O₃ are similar for both mechanisms and differ mainly in the absolute concentrations calculated. The higher solubility
of HO₂ compared to OH leads to a higher relative contribution of mass transfer and results in a higher absolute decrease of
HO₂. The consequent reduction in HO₂ concentration also leads to a reduced removal of NO_x by the formation of nitric acid
(HNO₃) and peroxy nitric acid (HNO₄). In combination with reduced OVOC concentrations, this results in generally higher
NO_x concentrations. Within the cloud droplet, O₂⁻ is in equilibrium with its conjugated base HO₂. Higher in-cloud HO₂
200 concentrations, caused by mass transfer and in-cloud OVOC oxidation, consequently lead to an increased destruction of O₃ via
Reaction R2. This results in an enhanced uptake of O₃ into the cloud droplet and an increased importance of cloud droplets as
O₃ sinks.

205 The impact of the new proposed mechanism is consistent with earlier box-model studies. The reduction in OVOCs is similar
to the findings given in Mouchel-Vallon et al. (2017) when using CLEPS. In contrast, the reduction in methylglyoxal differs
since in CLEPS, gas-phase methylglyoxal concentrations first increase and later decrease during the modelled cloud event
of Mouchel-Vallon et al. (2017). This difference is most likely linked to the usage of the intrinsic Henry's law constant and
the explicit representation of the methylglyoxal hydration/dehydration in JAMOC. Opposite to Mouchel-Vallon et al. (2017)
210 CAABA predicts a reduction in OH levels. However, this reduction in OH is in line with other modelling studies predicting a
similar reduction of gas-phase OH during cloud events (Tilgner et al., 2013). It is important to keep in mind that in Mouchel-
Vallon et al. (2017), a different cloud event is simulated, including different initial conditions and a different emission scenario.
In their study, the cloud forms after a certain time period, whereas in CAABA the cloud is present the whole time.

4 Model uncertainties

The uncertainties associated with the present kinetic model are mainly attributed to (1) assumptions and simplifications in the aqueous-phase mechanism, and (2) missing sinks of key oxidants. Each possible uncertainty is discussed in this section.

215 In general, aqueous-phase kinetics data suffer from many large uncertainties compared to the data available for the gas-phase. In the development of the implemented in-cloud oxidation scheme JAMOC, some assumptions are made that introduce modelling uncertainties. If rate constants are unknown, estimates are taken from Mouchel-Vallon et al. (2017). These are based on a structure-activity relationship (SAR) for the H-abstraction by OH for dissolved carbonyls and carboxylic acids considered in this study (Doussin and Monod, 2013). However, it is expected that the uncertainty in the estimated rate constants
220 is low since Doussin and Monod (2013) report that when evaluated using experimental data, their estimates were within ±20 % for 58 % of the calculated rate constants. Also the up-scaling of branching ratios to conserve mass, further influences the predictions of VOC oxidation. The mechanism should be updated with reaction rates and branching ratios as soon as



experimental results become available. The increased concentration and burden of certain organic acids heavily depend on the chemistry and solubility of some gem-diols. For example, the gas-phase oxidation of the methylglyoxal monohydrate leads to 225 the formation of pyruvic acid. The gas-phase production of pyruvic acid therefore depends on the mass transfer of this specific monohydrate. In the current implementation, the Henry's law constants for all gem-diols are estimated. For the methylglyoxal monohydrate, the estimated values range from 3.5×10^3 M atm $^{-1}$ to 2.4×10^4 M atm $^{-1}$.

In JAMOC, all soluble gas-phase VOCs not explicitly oxidised in clouds are still taken up into cloud droplets and removed by rainout (see Sect. 2.2). Arakaki et al. (2013) point out that by not taking the oxidation of all dissolved organic carbon (DOC) 230 into account, aqueous-phase OH concentrations might be overestimated. Based on observational estimates, they suggest a general scavenging rate constant of $k_{C,OH} = (3.8 \pm 1.9) \times 10^8$ M $^{-1}$ s $^{-1}$ for all DOC. If each DOC reacts with OH, the gas-phase concentration would be reduced, further influencing gas-phase VOC concentrations and the overall oxidation capacity. Implementing the DOC oxidation, suggested by Arakaki et al. (2013), for every scavenged DOC species would increase the aqueous-phase mechanism by more than 280 reactions, which is almost a doubling of the proposed organic mechanism. Within 235 the scope of this study, it is thus computationally not feasible to include this additional OH sink. Currently, the model run time increases from 5.64 s for EMACs minimum in-cloud oxidation scheme to 8.91 s for the new proposed mechanism JAMOC.

Reducing the model uncertainties introduced by estimates of Henry's law constants of gem-diols, and missing in-cloud DOC oxidation, is outside the scope of this study due to their complexity. Model representation of the latter is expected to influence the oxidation rate of VOCs in the cloud droplets and aerosols.

240 5 Conclusions

In this study, the new in-cloud oxidation scheme of soluble VOCs JAMOC is developed and implemented into MECCA. This mechanism is suitable for global model applications and based on the box-model mechanism CLEPS proposed by Mouchel-Vallou et al. (2017). The mechanism considers the phase transfer of OVOCs containing up to ten carbon atoms. For a selection 245 of OVOCs containing up to four carbon atoms, their acid/base and/or hydration/dehydration equilibria, and their reactions with OH, NO₃ and other oxidants (if available) are explicitly represented. Additionally, the gas-phase photo-oxidation of gem-diols and oxalic acid was implemented into the gas-phase mechanism MOM. Finally, JAMOC was tested within the CAABA box-model.

The proposed mechanism leads to a significant reduction in OVOCs and an overall reduction in important oxidants. These findings are in line with other box-model studies and demonstrate the importance of in-cloud chemistry in atmospheric chemistry. By not taking the in-cloud oxidation of OVOCs into account, global models will tend to overestimate the levels of OVOCs 250 and atmospheric oxidants. A complete analysis on the importance of JAMOC at a global scale is presented in Rosanka et al. (2020).



255 *Code availability.* The CAABA/MECCA model code is available as a community model published under the GNU General Public License (<http://www.gnu.org/copyleft/gpl.html>, last access: 30 July 2020). The model code can be found in the Supplement and in the code repository at <https://gitlab.com/RolfSander/caaba-mecca> (last access: 2 August 2020). In addition to the complete code, a list of chemical reactions including rate constants and references (meccanism.pdf) and a user manual (caaba_mecca_manual.pdf) are available in the manual directory of the supplement. A list of all Henry's law and accommodation constants (chemprop.pdf) is available in the tools/chemprop directory. For further information and updates, the CAABA/MECCA web page at <http://www.mecca.messy-interface.org> (last access: 30 July 2020) can be consulted.

260 *Author contributions.* SR and DT developed the chemical mechanism. The chemical mechanism was reviewed by RS. SR, DT, and RS implemented the mechanism into MECCA. The results were discussed by all co-authors. The manuscript was prepared by SR with the help of all co-authors.

Competing interests. The authors declare that they have no competing of interest.

265 *Acknowledgements.* The work described in this paper has received funding from the Initiative and Networking Fund of the Helmholtz Association through the project “Advanced Earth System Modelling Capacity (ESM)”. The content of this paper is the sole responsibility of the author(s) and it does not represent the opinion of the Helmholtz Association, and the Helmholtz Association is not responsible for any use that might be made of the information contained. The authors gratefully acknowledge the Earth System Modelling Project (ESM) for funding this work by providing computing time on the ESM partition of the supercomputer JUWELS at the Jülich Supercomputing Centre (JSC).



Table 1. Hydration constants (K_{hyd}), apparent (H^*) and intrinsic (H) Henry's law constants for aldehydes (see Sect. 2.2 for details). If not stated otherwise, hydration constants are obtained from Doussin and Monod (2013) and sources therein. If not stated otherwise, apparent Henry's law constants are taken from Burkholder et al. (2015).

Species	K_{hyd}	$H^* [\text{M/atm}]$	$H [\text{M/atm}]$
Formaldehyde	1278.0	3.23×10^3	2.53
Acetaldehyde	1.2	1.29×10^1	5.91
Glycolaldehyde	15.7	4.00×10^4	2.40×10^3
Glyoxal	350.0 ^a	4.19×10^5	1.19×10^3
Glyoxylic acid	1100.0	1.09×10^4	9.90
Methylglyoxal	2000.0	3.50×10^3 ^b	1.75

^a Ervens and Volkamer (2010)

^b Betterton and Hoffmann (1988)

Table 2. Initial box-model (CAABA) mixing ratios and emission rates for selected gas-phase species. Initial mixing ratios are a modified version of the scenario used by Taraborrelli et al. (2012).

Gas-phase species	Initial mixing ratio [nmol/mol]	Emission [mole. cm ⁻² s ⁻¹]
O ₃	30	-
NO	0.01	3.3×10^{-9}
NO ₂	0.1	-
HNO ₃	5.0×10^{-3}	-
H ₂ O ₂	7	-
CO	100	-
CO ₂	3.5×10^5	-
CH ₄	1.8×10^3	-
Formaldehyde	5	-
Methanol	0.5	-
Methyl peroxide	4	-
Formic acid	0.35	-
Acetic acid	2	-
Peroxy acetic acid	1.5	-
Hydroxy acetone	4	-
Methylglyoxal	0.5	-
Isoprene	0.1	-
Peroxyacetyl nitrate	0.1	-
Ethane	2	-

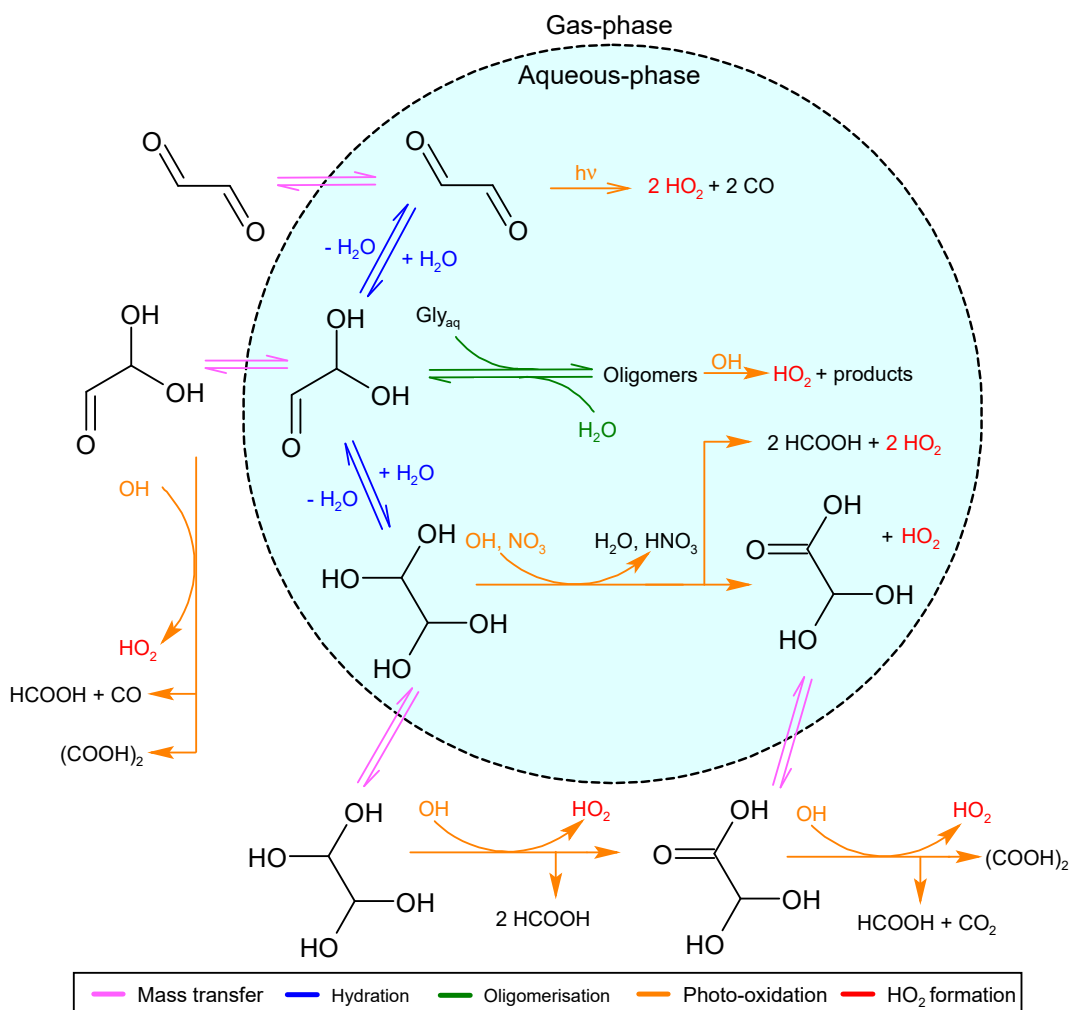


Figure 1. The chemical aqueous-phase mechanism of glyoxal (CHOCHO). The oxidation of the glyoxal dihydrate via OH and NO₃ is only represented. The oxidation via sulfate radical anions (SO₄⁻) is not shown. The oligomerisation of the glyoxal mono-hydrate occurs with glyoxal and its both hydrates (see Sect. 2.6). For simplicity Gly_{aq} donates all three species. Aqueous-phase glyoxal sources are not represented.

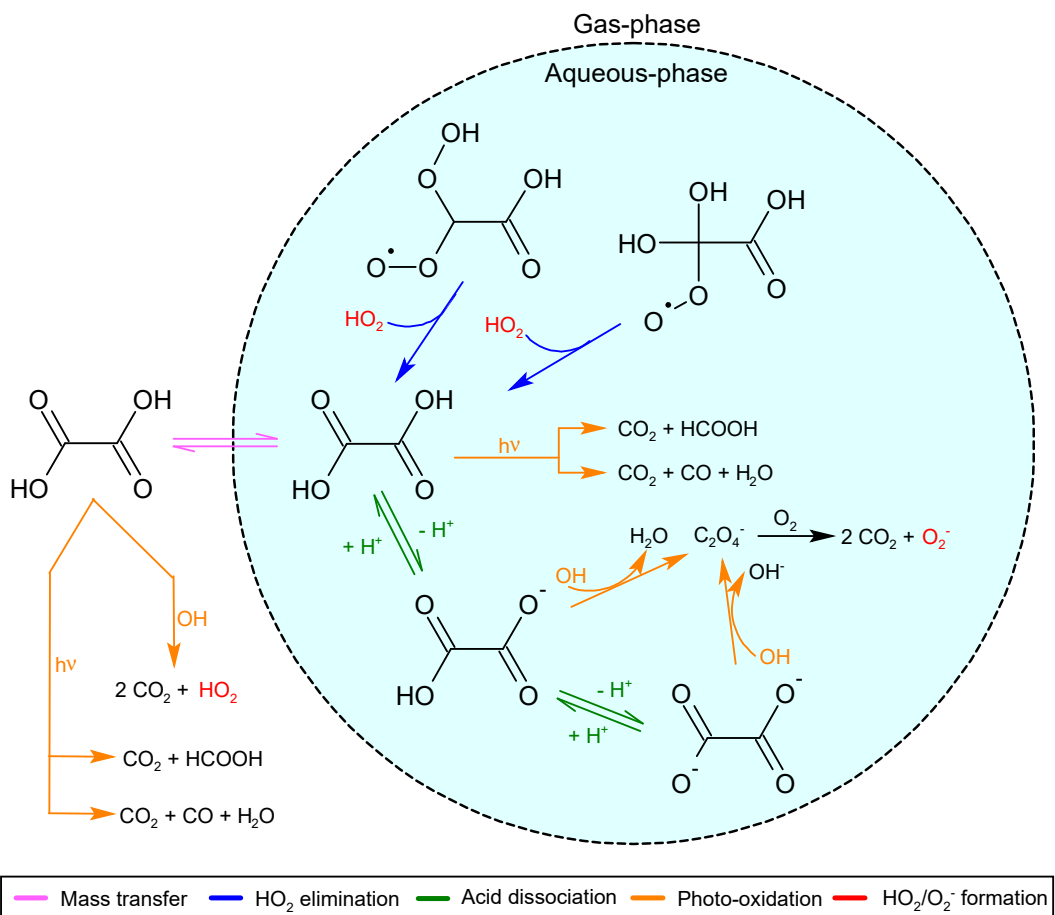


Figure 2. The chemical aqueous-phase mechanism of oxalic acid (HOOCCOOH). Only the oxidation via OH is represented. The oxidation via sulfate radical anions (SO_4^{2-}) is not shown.

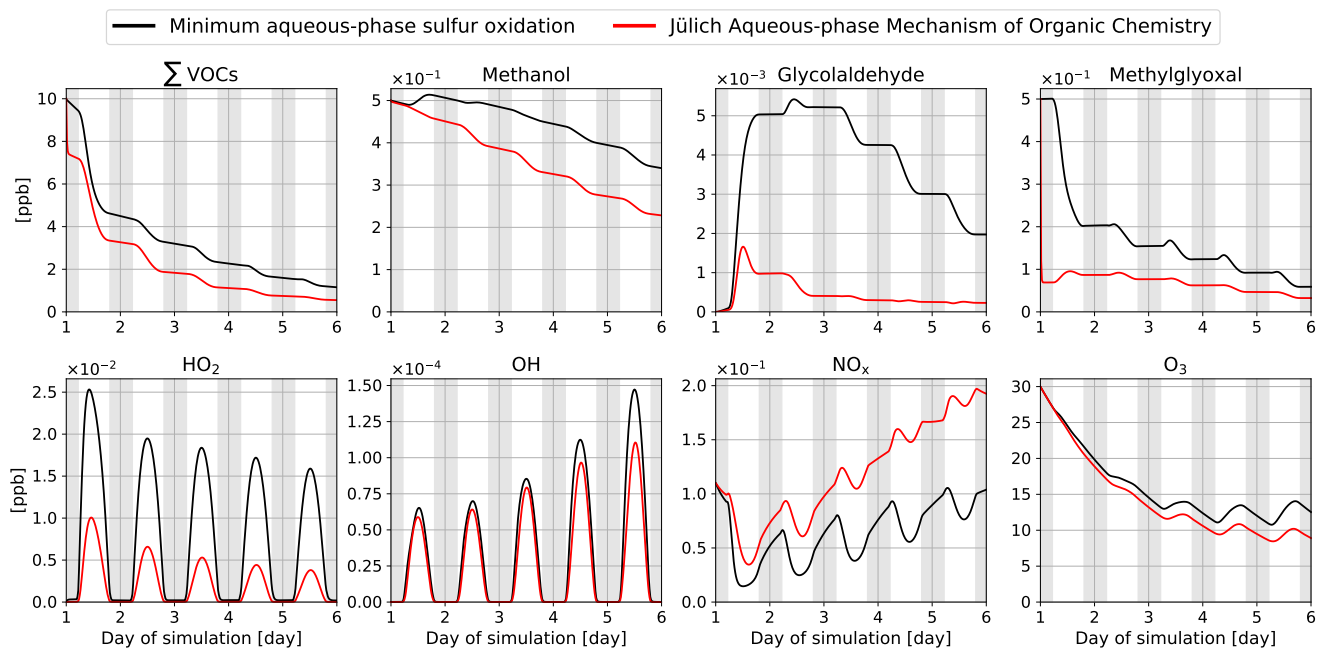


Figure 3. Time evolution for gas-phase mixing ratios of the sum of all the OVOCs explicitly oxidised in the proposed mechanism (\sum OVOCs = methanol + formaldehyde + methyl hydroperoxide + hydroxymethylhydroperoxide + ethanol + ethylene glycol + acetaldehyde + glycolaldehyde + glyoxal + hydroperoxide + methylglyoxal + isopropanol + isopropyl hydro peroxide + methacrolein + methyl vinyl ketone), methanol, glycolaldehyde, methylglyoxal, HO_2 , OH , NO_x , and O_3 within the boxmodel CAABA. Nighttime is indicated by a grey background shading. Mixing ratios are provided for two cases, one using the minimum aqueous-phase mechanism in global models (sulfur oxidation only, black line) and JAMOC (red line). Note that lines may overlap.



270 **References**

Arakaki, T., Anastasio, C., Kuroki, Y., Nakajima, H., Okada, K., Kotani, Y., Handa, D., Azechi, S., Kimura, T., Tsuhako, A., and Miyagi, Y.: A General Scavenging Rate Constant for Reaction of Hydroxyl Radical with Organic Carbon in Atmospheric Waters, *Environmental Science & Technology*, 47, 8196–8203, <https://doi.org/10.1021/es401927b>, 2013.

Back, R. A.: The ultraviolet absorption spectrum of oxalic acid vapor, *Canadian Journal of Chemistry*, 62, 1414–1428, <https://doi.org/10.1139/v84-241>, 1984.

Betterton, E. A. and Hoffmann, M. R.: Henry's law constants of some environmentally important aldehydes, *Environ. Sci. Technol.*, 22, 1415–1418, <https://doi.org/10.1021/ES00177A004>, 1988.

Bott, A. and Zdunkowski, W.: Electromagnetic energy within dielectric spheres, *J. Opt. Soc. Am. A*, 4, 1361–1365, <https://doi.org/10.1364/JOSAA.4.001361>, 1987.

Burkholder, J. B., Sander, S. P., Abbatt, J., Barker, J. R., Huie, R. E., Kolb, C. E., Kurylo, M. J., Orkin, V. L., Wilmouth, D. M., and Wine, P. H.: Chemical Kinetics and Photochemical Data for Use in Atmospheric Studies, Evaluation No. 18, JPL Publication 15-10, Jet Propulsion Laboratory, Pasadena, <http://jpldataeval.jpl.nasa.gov>, 2015.

Cabrera-Perez, D., Taraborrelli, D., Sander, R., and Pozzer, A.: Global atmospheric budget of simple monocyclic aromatic compounds, *Atmospheric Chemistry and Physics*, 16, 6931–6947, <https://doi.org/10.5194/acp-16-6931-2016>, 2016.

DeCosta, D. P. and Pincock, J. A.: Control of product distribution by Marcus type electron-transfer rates for the radical pair generated in benzylic ester photochemistry, *Journal of the American Chemical Society*, 111, 8948–8950, <https://doi.org/10.1021/ja00206a045>, 1989.

Doussin, J.-F. and Monod, A.: Structure–activity relationship for the estimation of OH-oxidation rate constants of carbonyl compounds in the aqueous phase, *Atmospheric Chemistry and Physics*, 13, 11 625–11 641, <https://doi.org/10.5194/acp-13-11625-2013>, 2013.

Epstein, S. A. and Nizkorodov, S. A.: A comparison of the chemical sinks of atmospheric organics in the gas and aqueous phase, *Atmospheric Chemistry and Physics*, 12, 8205–8222, <https://doi.org/10.5194/acp-12-8205-2012>, 2012.

Ervens, B.: Modeling the Processing of Aerosol and Trace Gases in Clouds and Fogs, *Chemical Reviews*, 115, 4157–4198, <https://doi.org/10.1021/cr5005887>, 2015.

Ervens, B. and Volkamer, R.: Glyoxal processing by aerosol multiphase chemistry: towards a kinetic modeling framework of secondary organic aerosol formation in aqueous particles, *Atmospheric Chemistry and Physics*, 10, 8219–8244, <https://doi.org/10.5194/acp-10-8219-2010>, 2010.

Ervens, B., Renard, P., Tlili, S., Ravier, S., Clément, J.-L., and Monod, A.: Aqueous-phase oligomerization of methyl vinyl ketone through photooxidation – Part 2: Development of the chemical mechanism and atmospheric implications, *Atmospheric Chemistry and Physics*, 15, 9109–9127, <https://doi.org/10.5194/acp-15-9109-2015>, 2015.

Hahnenstein, I., Albert, M., Hasse, H., Kreiter, C. G., and Maurer, G.: NMR Spectroscopic and Densimetric Study of Reaction Kinetics of Formaldehyde Polymer Formation in Water, Deuterium Oxide, and Methanol, *Industrial & Engineering Chemistry Research*, 34, 440–450, <https://doi.org/10.1021/ie00041a003>, 1995.

Hens, K., Novelli, A., Martinez, M., Auld, J., Axinte, R., Bohn, B., Fischer, H., Keronen, P., Kubistin, D., Nölscher, A. C., Oswald, R., Paasonen, P., Petäjä, T., Regelin, E., Sander, R., Sinha, V., Sipilä, M., Taraborrelli, D., Tatum Ernest, C., Williams, J., Lelieveld, J., and Harder, H.: Observation and modelling of HO_x radicals in a boreal forest, *Atmospheric Chemistry and Physics*, 14, 8723–8747, <https://doi.org/10.5194/ACP-14-8723-2014>, 2014.



Herrmann, H.: Kinetics of Aqueous Phase Reactions Relevant for Atmospheric Chemistry, *Chemical Reviews*, 103, 4691–4716, <https://doi.org/10.1021/cr020658q>, 2003.

Herrmann, H., Schaefer, T., Tilgner, A., Styler, S. A., Weller, C., Teich, M., and Otto, T.: Tropospheric Aqueous-Phase Chemistry: Kinetics, Mechanisms, and Its Coupling to a Changing Gas Phase, *Chemical Reviews*, 115, 4259–4334, <https://doi.org/10.1021/cr500447k>, pMID: 310 25950643, 2015.

Hilborn, J. W. and Pincock, J. A.: Rates of decarboxylation of acyloxy radicals formed in the photolysis of substituted 1-naphthylmethyl alkanoates, *Journal of the American Chemical Society*, 113, 2683–2686, <https://doi.org/10.1021/ja00007a049>, 1991.

Jenkin, M. E., Young, J. C., and Rickard, A. R.: The MCM v3.3.1 degradation scheme for isoprene, *Atmospheric Chemistry and Physics*, 15, 11 433–11 459, <https://doi.org/10.5194/acp-15-11433-2015>, 2015.

Jöckel, P., Tost, H., Pozzer, A., Brühl, C., Buchholz, J., Ganzeveld, L., Hoor, P., Kerkweg, A., Lawrence, M. G., Sander, R., Steil, B., Stiller, G., Tanarhte, M., Taraborrelli, D., van Aardenne, J., and Lelieveld, J.: The atmospheric chemistry general circulation model ECHAM5/MESSy1: consistent simulation of ozone from the surface to the mesosphere, *Atmospheric Chemistry and Physics*, 6, 5067–5104, <https://doi.org/10.5194/acp-6-5067-2006>, 2006.

Jöckel, P., Kerkweg, A., Pozzer, A., Sander, R., Tost, H., Riede, H., Baumgaertner, A., Gromov, S., and Kern, B.: Development cycle 2 of the 320 Modular Earth Submodel System (MESSy2), *Geoscientific Model Development*, 3, 717–752, <https://doi.org/10.5194/gmd-3-717-2010>, 2010.

Jöckel, P., Tost, H., Pozzer, A., Kunze, M., Kirner, O., Brenninkmeijer, C. A. M., Brinkop, S., Cai, D. S., Dyroff, C., Eckstein, J., Frank, F., Garny, H., Gottschaldt, K.-D., Graf, P., Grewe, V., Kerkweg, A., Kern, B., Matthes, S., Mertens, M., Meul, S., Neumaier, M., Nützel, M., Oberländer-Hayn, S., Ruhnke, R., Runde, T., Sander, R., Scharffe, D., and Zahn, A.: Earth System Chemistry integrated Modelling (ESCiMo) with the Modular Earth Submodel System (MESSy) version 2.51, *Geoscientific Model Development*, 9, 1153–1200, 325 <https://doi.org/10.5194/gmd-9-1153-2016>, 2016.

Jülich Supercomputing Centre: JUWELS: Modular Tier-0/1 Supercomputer at the Jülich Supercomputing Centre, *Journal of large-scale research facilities*, 5, <https://doi.org/10.17815/jlsrf-5-171>, 2019.

Lim, Y. B., Tan, Y., and Turpin, B. J.: Chemical insights, explicit chemistry, and yields of secondary organic aerosol from OH radical oxidation 330 of methylglyoxal and glyoxal in the aqueous phase, *Atmospheric Chemistry and Physics*, 13, 8651–8667, <https://doi.org/10.5194/acp-13-8651-2013>, 2013.

Mayer, B. and Madronich, S.: Actinic flux and photolysis in water droplets: Mie calculations and geometrical optics limit, *Atmospheric Chemistry and Physics*, 4, 2241–2250, <https://doi.org/10.5194/acp-4-2241-2004>, 2004.

Monod, A., Chevallier, E., Jolibois, R. D., Doussin, J., Picquet-Varrault, B., and Carlier, P.: Photooxidation of methylhydroperoxide 335 and ethylhydroperoxide in the aqueous phase under simulated cloud droplet conditions, *Atmospheric Environment*, 41, 2412 – 2426, <https://doi.org/10.1016/j.atmosenv.2006.10.006>, 2007.

Mouchel-Vallon, C., Deguillaume, L., Monod, A., Perroux, H., Rose, C., Ghigo, G., Long, Y., Leriche, M., Aumont, B., Patry, L., Armand, P., and Chaumerliac, N.: CLEPS 1.0: A new protocol for cloud aqueous phase oxidation of VOC mechanisms, *Geoscientific Model Development*, 10, 1339–1362, <https://doi.org/10.5194/gmd-10-1339-2017>, 2017.

Nölscher, A., Butler, T., Auld, J., Veres, P., Muñoz, A., Taraborrelli, D., Vereecken, L., Lelieveld, J., and Williams, J.: Using 340 total OH reactivity to assess isoprene photooxidation via measurement and model, *Atmos. Environ.*, 89, 453–463, <https://doi.org/10.1016/j.atmosenv.2014.02.024>, 2014.



Piesiak, A., Schuchmann, M. N., Zegota, H., and von Sonntag, C.: β -Hydroxyethylperoxy radicals: a study of the γ -radiolysis and pulse radiolysis of ethylene in oxygenated aqueous solutions, *Z. Naturforsch.*, 39, 1262–1267, 1984.

345 Poulain, L., Katrib, Y., Isikli, E., Liu, Y., Wortham, H., Mirabel, P., Calvé, S. L., and Monod, A.: In-cloud multiphase behaviour of acetone in the troposphere: Gas uptake, Henry's law equilibrium and aqueous phase photooxidation, *Chemosphere*, 81, 312 – 320, <https://doi.org/10.1016/j.chemosphere.2010.07.032>, 2010.

Rosanka, S., Sander, R., Franco, B., Wespes, C., Wahner, A., and Taraborrelli, D.: Oxidation of low-molecular weight organic compounds in cloud droplets: global impact on tropospheric oxidants, *Atmospheric Chemistry and Physics Discussions*, submitted companion paper, 350 acp-2020-1041, 2020.

Ruggaber, A., Dlugi, R., Bott, A., Forkel, R., Herrmann, H., and Jacobi, H.-W.: Modelling of radiation quantities and photolysis frequencies in the aqueous phase in the troposphere, *Atmospheric Environment*, 31, 3137 – 3150, [https://doi.org/10.1016/S1352-2310\(97\)00058-7](https://doi.org/10.1016/S1352-2310(97)00058-7), eUMAC: European Modelling of Atmospheric Constituents, 1997.

Rumble, J. R., ed.: CRC Handbook of Chemistry and Physics, 101st Edition, CRC Press, Boca Raton, FL, 2020.

355 Sander, R.: Modeling Atmospheric Chemistry: Interactions between Gas-Phase Species and Liquid Cloud/Aerosol Particles, *Surveys in Geophysics*, 20, 1–31, <https://doi.org/10.1023/A:1006501706704>, 1999.

Sander, R.: Compilation of Henry's law constants (version 4.0) for water as solvent, *Atmospheric Chemistry and Physics*, 15, 4399–4981, <https://doi.org/10.5194/acp-15-4399-2015>, 2015.

360 Sander, R., Jöckel, P., Kirner, O., Kunert, A. T., Landgraf, J., and Pozzer, A.: The photolysis module JVAL-14, compatible with the MESSY standard, and the JVal PreProcessor (JVPP), *Geoscientific Model Development*, 7, 2653–2662, <https://doi.org/10.5194/gmd-7-2653-2014>, 2014.

Sander, R., Baumgaertner, A., Cabrera-Perez, D., Frank, F., Gromov, S., Groß, J.-U., Harder, H., Huijnen, V., Jöckel, P., Karydis, V. A., Niemeyer, K. E., Pozzer, A., Riede, H., Schultz, M. G., Taraborrelli, D., and Tauer, S.: The community atmospheric chemistry box model CAABA/MECCA-4.0, *Geoscientific Model Development*, 12, 1365–1385, <https://doi.org/10.5194/gmd-12-1365-2019>, 2019.

365 Schuchmann, M. N., Zegota, H., and von Sonntag, C.: Acetateperoxy radicals, $O_2CH_2CO_2^-$: a study on the γ -radiolysis and pulse radiolysis of acetate in oxygenated aqueous solutions, *Z. Naturforsch. Pt. B*, 40, 215–221, 1985.

Schwartz, S. E.: Mass-Transport Considerations Pertinent to Aqueous Phase Reactions of Gases in Liquid-Water Clouds, in: *Chemistry of Multiphase Atmospheric Systems*, edited by Jaeschke, W., pp. 415–471, Springer Berlin Heidelberg, Berlin, Heidelberg, 1986.

370 Staehelin, J. and Hoigné, J.: Decomposition of ozone in water in the presence of organic solutes acting as promoters and inhibitors of radical chain reactions, *Environmental Science & Technology*, 19, 1206–1213, <https://doi.org/10.1021/es00142a012>, 1985.

Staehelin, J., Buehler, R. E., and Hoigné, J.: Ozone decomposition in water studied by pulse radiolysis. 2. Hydroxyl and hydrogen tetroxide (HO_4) as chain intermediates, *The Journal of Physical Chemistry*, 88, 5999–6004, <https://doi.org/10.1021/j150668a051>, 1984.

Taraborrelli, D., Lawrence, M. G., Butler, T. M., Sander, R., and Lelieveld, J.: Mainz Isoprene Mechanism 2 (MIM2): an isoprene oxidation mechanism for regional and global atmospheric modelling, *Atmospheric Chemistry and Physics*, 9, 2751–2777, 375 <https://doi.org/10.5194/ACP-9-2751-2009>, 2009.

Taraborrelli, D., Lawrence, M. G., Crowley, J. N., Dillon, T. J., Gromov, S., Groß, C. B. M., Vereecken, L., and Lelieveld, J.: Hydroxyl radical buffered by isoprene oxidation over tropical forests, *Nature Geoscience*, 5, 190–193, <https://doi.org/10.1038/ngeo1405>, 2012.

Tilgner, A., Bräuer, P., Wolke, R., and Herrmann, H.: Modelling multiphase chemistry in deliquescent aerosols and clouds using CAPRAM3.0i, *Journal of Atmospheric Chemistry*, 70, 221–256, <https://doi.org/10.1007/s10874-013-9267-4>, 2013.



380 Tost, H., Jöckel, P., Kerkweg, A., Sander, R., and Lelieveld, J.: Technical note: A new comprehensive SCAVenging submodel for global atmospheric chemistry modelling, *Atmospheric Chemistry and Physics*, 6, 565–574, <https://doi.org/10.5194/acp-6-565-2006>, 2006.

Tost, H., Jöckel, P., Kerkweg, A., Pozzer, A., Sander, R., and Lelieveld, J.: Global cloud and precipitation chemistry and wet deposition: tropospheric model simulations with ECHAM5/MESSy1, *Atmospheric Chemistry and Physics*, 7, 2733–2757, <https://doi.org/10.5194/acp-7-2733-2007>, 2007.

385 United States Environmental Protection Agency: Estimation Programs Interface Suite™ for Microsoft® Windows, Washington, DC, USA, 2012.

Villalta, P. W., Lovejoy, E. R., and Hanson, D. R.: Reaction probability of peroxyacetyl radical on aqueous surfaces, *Geophysical Research Letters*, 23, 1765–1768, <https://doi.org/10.1029/96GL01286>, 1996.

von Sonntag, C.: The chemical basis of radiation biology, Taylor & Francis London, 1987.

390 von Sonntag, C. and Schuchmann, H.-P.: Peroxyl Radicals in Aqueous Solutions, in: *The Chemistry of Free Radicals: Peroxyl Radicals*, Wiley, New York, 1997.

Yamamoto, S. and Back, R. A.: The gas-phase photochemistry of oxalic acid, *The Journal of Physical Chemistry*, 89, 622–625, <https://doi.org/10.1021/j100250a014>, 1985.

Zegota, H., Schuchmann, M. N., Schulz, D., and von Sonntag, C.: Acetonylperoxy radicals, $\text{CH}_3\text{COCH}_2\text{O}_2$: A study on the γ -radiolysis
395 and pulse radiolysis of acetone in oxygenated aqueous solutions, *Z. Naturforsch.*, 41, 1015–1022, 1986.